

Passively Q-switched operation of a 1.94 μm thulium-doped solid-state laser based on MXene V_2CT_x

Jinhe Yuan (袁晋鹤)¹, Jiarui Li (李佳睿)¹, Zhengyang Wu (吴政阳)², Shuangcheng Li (李双成)², Jie Han (韩杰)^{3*}, and Linjun Li (李林军)^{2**}

¹College of Physical Science and Technology, Heilongjiang University, Harbin 150080, China

²Heilongjiang Provincial Key Laboratory of Laser Spectroscopy Technology and Application, Harbin University of Science and Technology, Harbin 150080, China

³School of Data Science and Technology, Heilongjiang University, Harbin 150080, China

*Corresponding author: 2002136@hlju.edu.cn

**Corresponding author: llj7897@126.com

Received March 31, 2022 | Accepted August 12, 2022 | Posted Online September 16, 2022

MXene V_2CT_x has great practicability because it is not easy to degrade under ambient conditions. In this paper, a V_2CT_x saturable absorber (SA) was firstly applied to a passively Q-switched (PQS) laser, to the best of our knowledge. The V_2CT_x -SA was prepared by the spin-coating method. The linear absorption of the V_2CT_x -SA in the 1000–2200 nm region and the nonlinear absorption near 2 μm were studied. With the V_2CT_x -SA, a typical PQS operation at 1.94 μm was realized in a Tm:YAlO₃ laser. The minimum pulse width produced by the PQS laser was 528 ns, and the peak power, repetition rate, and average output power were 10.06 W, 65.9 kHz, and 350 mW, respectively. Meanwhile, the maximum pulse energy was 6.33 μJ . This work demonstrates that the V_2CT_x can be used as an effective SA to obtain nanosecond pulses with high peak power and high repetition rate simultaneously.

Keywords: passive Q-switching; MXene V_2CT_x ; saturable absorber; thulium doping.

DOI: 10.3788/COL202321.021402

1. Introduction

Nanosecond pulsed lasers based on thulium-doped solid-state lasers and emission in the 1.9–2 μm band ($^3\text{F}_4 \rightarrow ^3\text{H}_6$) have wide application values in laser ranging, spectroscopy, optical medicine, and metrology^[1–4]. In the past two decades, passively Q-switched (PQS) lasers using saturable absorbers (SAs) have strongly promoted the development of high-quality pulsed lasers, largely due to the rapid development of SAs. Therefore, it is very important to explore high-performance SAs to improve the performance of the PQS laser. In the past, Cr:ZnS^[5], Cr:ZnSe^[6], and semiconductor SA mirrors (SESAMs)^[7] have been widely used as SAs in the wavelength region of 1.9–2 μm . However, the disadvantages of SESAMs, such as complex manufacturing, high cost, and narrow absorption band width, greatly limit the application. Cr:ZnS and Cr:ZnSe have large absorption cross sections and are very suitable for generating high-energy pulsed lasers. The PQS thulium-doped lasers based on Cr:ZnSe and Cr:ZnS have been proved to be able to obtain millijoule pulse lasers; however, the corresponding repetition rates are rather low^[5,6].

In the recent years, SAs based on two-dimensional (2D) materials, including graphene^[8], black phosphorus (BP)^[9], transition metal dichalcogenide (TMD)^[10], topological insulators, and

MXene^[11,12], have been widely investigated due to their excellent saturable absorption properties. Moreover, MXene also exhibits large optical modulation depth, high damage threshold, excellent conductivity, tunable bandgap, high electric capacity, and so on^[13–17].

Recently, a few MXenes ($\text{Ti}_3\text{C}_2\text{T}_x$, Ti_2CT_x , $\text{Ti}_4\text{N}_3\text{T}_x$, Nb_2CT_x) have been applied to pulse lasers with different working mechanisms^[18–22]. In 2019, a $\text{Ti}_3\text{C}_2\text{T}_x$ Q-switched Tm, Gd:CaF₂ laser with 2.4 μs pulse width was reported by Zu *et al.*, whose working wavelength was 1974.5 or 1929.7 nm, which mainly depended on the transmittance of the output coupler (OC)^[19]. In 2021, Huang *et al.* demonstrated that Ti_2CT_x could be a promising SA in a 1.06 μm Nd:Y₃Al₅O₁₂ (Nd:YAG) solid-state laser^[20]. In 2020 and 2021, solid-state PQS Er:Lu₂O₃ lasers at 2.85 μm with $\text{Ti}_4\text{N}_3\text{T}_x$ and Nb_2CT_x SAs were achieved, respectively^[21,22]. However, common MXenes such as Ti_2CT_x and $\text{Ti}_3\text{C}_2\text{T}_x$ have the disadvantage of easy degradation under ambient conditions, so their practical application is greatly limited^[3,23]. Fortunately, V_2CT_x nanosheets have better stability than $\text{Ti}_3\text{C}_2\text{T}_x$ and Ti_2CT_x nanosheets^[23].

In 2020, MXene V_2CT_x was first used as an SA in a 1.56 μm mode-locked fiber laser, showing excellent saturable absorption

performance^[23]. However, the saturable absorption behavior of V_2CT_x -SA in a Q-switched laser has not been studied. Compared with a fiber laser, a solid-state laser has smaller nonlinear pulse splitting^[24], so the research of the V_2CT_x Q-switched solid-state laser is of great significance to obtain high-energy short pulses.

In this paper, the linear and nonlinear absorption properties of a home-made V_2CT_x -SA were studied. With the V_2CT_x -SA, a typical PQS operation at 1.94 μm was realized in a Tm:YAlO₃ (Tm:YAP) laser. To the best of our knowledge, the first demonstration of a V_2CT_x Q-switched laser is reported in this paper.

2. Preparation and Characteristics of V_2CT_x -SA

The multilayer V_2CT_x powder (10 mg) and anhydrous ethanol (10 mg) were mixed together in a glass bottle, and ultrasound was used in an ultrasound machine for 1 h. We then used a rotary coater (KW-4A, Chinese Academy of Sciences) to coat the V_2CT_x solution on one side of the quartz plate. Based on the above operation, a home-made V_2CT_x -SA was ready. The surface structure of V_2CT_x nanosheets was captured at 1000 \times magnification, as shown in Fig. 1(a). The component of V_2CT_x nanosheets is shown in Fig. 1(b), which was analyzed by energy dispersive spectroscopy (EDS). The oxygen and fluorine peaks indicated the generation of numerous surface termination groups, and the weak aluminum peak represented some residue of V_2AlC . The linear absorption of the V_2CT_x -SA at 1000–2200 nm is shown in Fig. 1(c). The presence of surface functional groups is the main cause of the broadband absorption spectrum^[18,25]. Figure 1(d) shows the relationship between nonlinear absorption and optical intensity. The experimental data were measured by a home-made Tm³⁺-Ho³⁺ co-doped laser (2119.3 nm, 55 ns, 10 kHz). The fitting curve was obtained by the following formula:

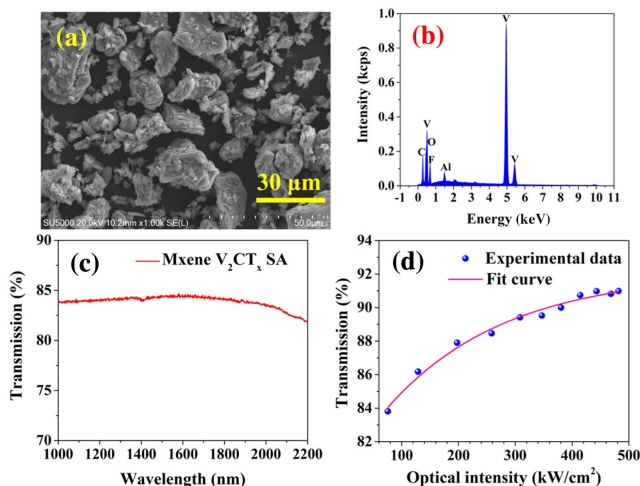


Fig. 1. (a) Electron image of V_2CT_x , (b) EDS of V_2CT_x , (c) linear absorption spectrum of V_2CT_x -SA, and (d) nonlinear absorption property of V_2CT_x -SA.

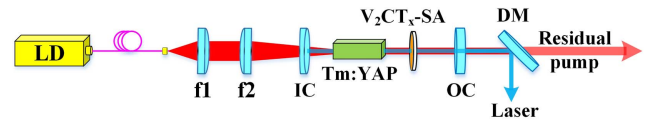


Fig. 2. Setup of the PQS Tm:YAP laser. V_2CT_x -SA, V_2CT_x saturable absorber; IC, input coupler; OC, output coupler; DM, dichroic mirror; f1 and f2, convex lenses.

$$T(I) = 1 - \Delta T \cdot \exp\left(\frac{-I}{I_{\text{sat}}}\right) - T_{\text{ns}}.$$

Herein, I and T are the optical intensity and transmittance, and the calculated non-saturated absorption loss (T_{ns}), saturation intensity (I_{sat}), and modulation depth (ΔT) were 7.9%, 208.95 kW/cm², and 11.6%, respectively.

The measurement results show that V_2CT_x -SA has the advantage of large modulation depth, so it is very suitable for obtaining high energy and short pulse width.

3. Experiment Setup

Figure 2 shows the experiment setup. The pump laser was a 793 nm laser diode (LD). After passing through the lenses f1 (25 mm) and f2 (50 mm), the pump spot in the Tm:YAP crystal was 210 μm . The size of the crystal (b -axis cut, 3% doping concentration) was 3 mm \times 3 mm \times 8 mm. The heat generated in the crystal can be taken away in time by a water cooler to ensure the operating temperature is 286 K. In this experiment, a dual mirror linear resonator was used to carry out the study, and the physical cavity length was 38 mm. The input coupler (IC) was a flat concave mirror, and its curve radius was 100 mm. Three OCs (plane mirror) were used here, and the transmittances (T) at 1900–2100 nm were 1.5%, 2.5%, and 5.0%, respectively. The generated laser was separated by the dichroic mirror (DM). The prepared V_2CT_x -SA was inserted between the OC and Tm:YAP crystal, which served as the Q-switch. The laser radii on the Tm:YAP crystal and V_2CT_x -SA were 187 and 174 μm , respectively.

4. Results and Discussion

Figure 3(a) shows the average output power obtained in the PQS mode. When the incident power was increased to 4.26, 5.01, and 4.25 W, respectively, the PQS laser with the OC of $T = 1.5\%$, 2.5%, and 5.0% started the Q-switching operation. The maximum average output power available was 190, 220, and 350 mW, corresponding to the slope efficiencies of 3.5%, 4.4%, and 6.3%, respectively.

For comparison with the PQS mode, the continuous-wave (CW) output power obtained with the 5.0% output mirror was also studied. Up to 1.48 W output power with a slope efficiency of 20.5% was achieved, and the laser threshold was approximately 1.6 W, as shown in Fig. 3(b). Compared with the CW mode, the laser threshold of the PQS laser increased, and the output power decreased, which can be attributed to

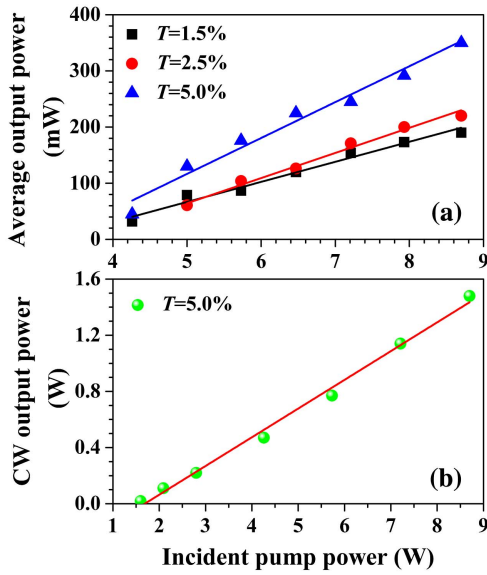


Fig. 3. Relationship between output power and incident pump power: (a) PQS operation and (b) CW operation.

the insertion loss of the SA. Figure 4 shows the pulse characteristics achieved in PQS mode. By using the OC of $T = 5.0\%$, a shortest pulse width of 528 ns with a 65.9 kHz repetition rate was obtained. By using the OCs of $T = 1.5\%$ and 2.5% , the minimum pulse widths were 636 and 919 ns, and the maximum repetition rates were 69.3 and 74.6 kHz. The pulse energy tends to be constant, as shown in Fig. 5(a), while the peak power increases roughly linearly, as shown in Fig. 5(b). The maximum pulse energy and peak power were 6.33 μJ and 10.06 W, which were obtained at the pump power of 7.21 and 8.69 W,

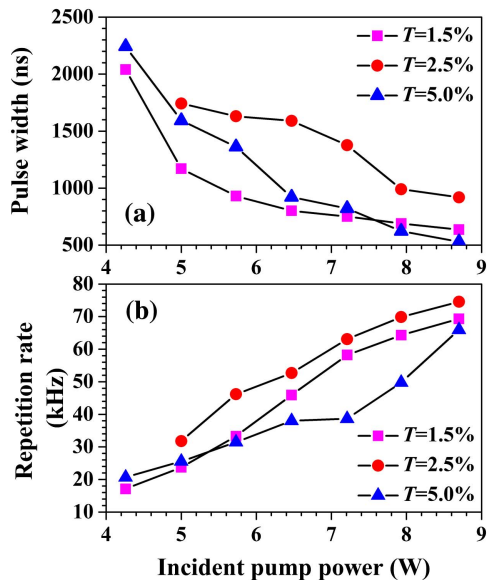


Fig. 4. Performances of V_2CT_x Q-switched laser: (a) pulse width and (b) repetition rate versus the incident pump power.

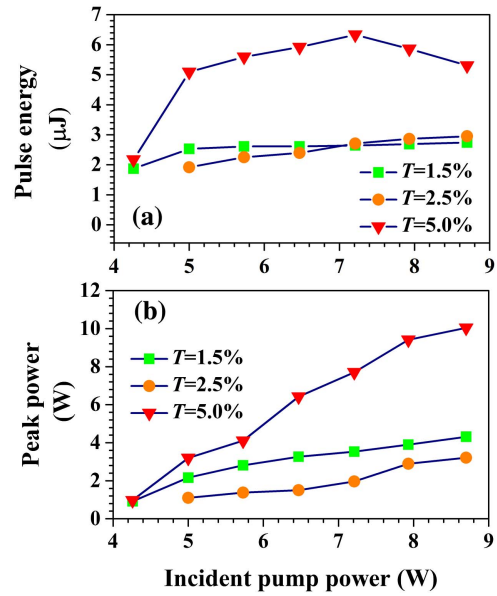


Fig. 5. Performances of V_2CT_x Q-switched laser: (a) pulse energy and (b) peak power versus the incident pump power.

respectively. By using the OCs of $T = 1.5\%$ and 2.5% , the maximum pulse energies of 2.74 and 2.95 μJ were obtained, and the corresponding peak powers were 4.31 and 3.21 W, respectively.

If we continue to increase the incident pump power, the SA will be destroyed with the 1.5% output mirror. Therefore, we can infer the damage threshold of MXene- V_2CT_x based on the intracavity energy, and its value is estimated to be 0.42 J/cm^2 . By comparing the laser performance of the three output mirrors, it can be concluded that the optimum performance was achieved with the 5.0% output mirror, that is, smaller pulse width and repetition rate as well as higher energy and peak power can be obtained.

Figure 6 shows the temporal profiles and pulse trains obtained under different conditions. With the 5.0% output mirror, the measured output spectra are shown in Fig. 7. When the incident pump powers were 5.73 and 8.69 W, the peak emission wavelengths in the CW operation were 1992.1 and 1991.7 nm, corresponding to the linewidths of 4.7 and 5.6 nm, respectively. The peak emission wavelengths were decreased to 1937.8 and 1937.4 nm in the PQS operation, and the corresponding linewidths were 1.1 and 2.2 nm, respectively.

The shift of laser wavelengths from CW operation to PQS operation is due to the fact that the excited-state population fraction in PQS operation is much higher than that in CW operation, which results in the peak of the gain cross section moving to the shorter wavelength. Also, the linewidths of PQS operation are narrower than those of CW operation, which can be mainly attributed to the etalon effect caused by the SA mirror. The beam quality of the PQS laser at 350 mW output power was evaluated by a BP109-IR2M beam profiler. The measured M^2 factor in the X direction was 1.15, and the value in the Y direction was 1.18, which are shown in Fig. 8(a). The spatial distributions of the beam are shown in Figs. 8(b) and 8(c).

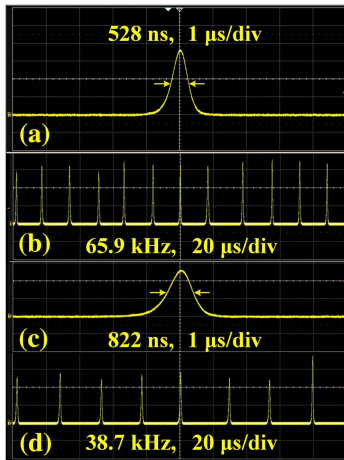


Fig. 6. Typical temporal profiles and pulse trains. (a) and (b) are recorded at the peak power of 10.06 W, and (c) and (d) are recorded at the pulse energy of 6.33 μ J.

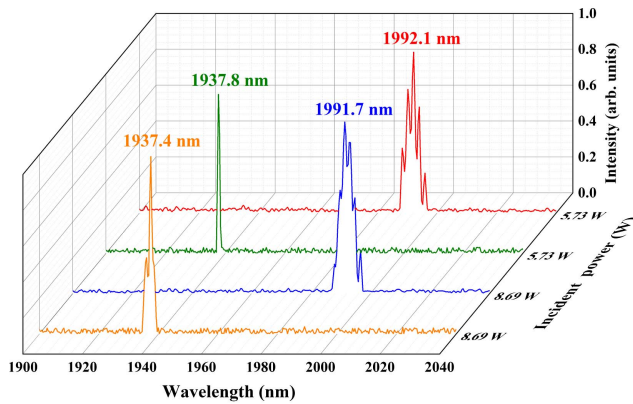


Fig. 7. CW spectra with a peak wavelength of 1992.1 and 1991.7 nm, and PQS spectra with a peak wavelength of 1937.8 and 1937.4 nm.

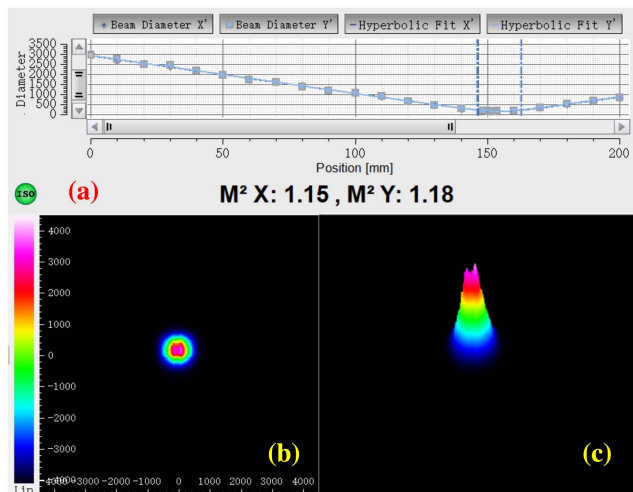


Fig. 8. (a) Measured M^2 factor, and (b) and (c) are 2D and 3D spatial power distributions, respectively.

5. Conclusion

In summary, a multilayer V_2CT_x -SA was prepared. The linear and nonlinear absorption properties of the SA were characterized. By using the V_2CT_x -SA in a Tm:YAP laser, a typical PQS operation at 1.94 μ m was realized. The optimum performance was achieved with the 5.0% output mirror. At a repetition rate of 65.9 kHz, the maximum peak power and average output power were 10.06 W and 350 mW, respectively, corresponding to the minimum pulse width of 528 ns. Maximum pulse energy of 6.33 μ J was achieved at the 38.7 kHz repetition rate. Furthermore, the obtained M^2 factor was less than 1.2.

Acknowledgement

This work was supported by the China Postdoctoral Science Foundation (No. 2020M670937) and the Basic Scientific Research Business Expenses of Colleges and Universities in Heilongjiang Province (No. 2021-KYYWF-0020).

References

1. A. Godard, "Infrared (2–12 μ m) solid-state laser sources: a review," *C. R. Phys.* **8**, 1100 (2007).
2. T. Bach, T. R. W. Herrmann, A. Haecker, M. S. Michel, and A. Gross, "Thulium:yttrium-aluminium-garnet laser prostatectomy in men with refractory urinary retention," *BJU Int.* **104**, 361 (2009).
3. Z. Niu, T. Feng, T. Li, K. Yang, J. Zhao, G. Li, D. Li, S. Zhao, W. Qiao, H. Chu, and Y. Liu, "Theoretical and experimental investigations on doubly Q-switched Tm:YAP laser with EOM and Sb_2Te_3 nanosheets," *Opt. Express* **29**, 24684 (2021).
4. R. Thouroude, A. Tyazhev, A. Hideur, P. Loiko, P. Camy, J. L. Doualan, H. Gilles, and M. Laroche, "Widely tunable in-band-pumped Tm:CaF₂ laser," *Opt. Lett.* **45**, 4511 (2020).
5. D. Sebbag, A. Korenfeld, U. Ben-Ami, D. Elooz, E. Shalom, and S. Noach, "Diode end-pumped passively Q-switched Tm:YAP laser with 1.85-mJ pulse energy," *Opt. Lett.* **40**, 1250 (2015).
6. A. Korenfeld, D. Sebbag, U. Ben-Ami, E. Shalom, G. Marcus, and S. Noach, "High pulse energy passive Q-switching of a diode-pumped Tm:YLF laser by Cr:ZnSe," *Laser Phys. Lett.* **12**, 045804 (2015).
7. U. Keller, "Recent developments in compact ultrafast lasers," *Nature* **424**, 831 (2003).
8. J. Ma, G. Xie, J. Zhang, P. Yuan, D. Tang, and L. Qian, "Passively mode-locked Tm:YAG ceramic laser based on grapheme," *IEEE J. Sel. Top. Quantum Electron.* **21**, 50 (2015).
9. J. Sotor, G. Sobon, M. Kowalczyk, W. Macherzynski, P. Paletko, and K. M. Abramski, "Ultrafast thulium-doped fiber laser mode locked with black phosphorus," *Opt. Lett.* **40**, 3885 (2015).
10. L. Li, W. Cui, X. Yang, L. Zhou, Y. Yang, W. Xie, X. Duan, Y. Shen, and J. Han, "A high-beam-quality passively Q-switched 2 μ m solid-state laser with a WSe₂ saturable absorber," *Opt. Laser Technol.* **125**, 105960 (2020).
11. B. Guo, Q. L. Xiao, S. H. Wang, and H. Zhang, "2D layered materials: synthesis, nonlinear optical properties, and device applications," *Laser Photonics Rev.* **13**, 1800327 (2019).
12. J. Zou, Q. Ruan, X. Zhang, B. Xu, Z. Cai, and Z. Luo, "Visible-wavelength pulsed lasers with low-dimensional saturable absorbers," *Nanophotonics* **9**, 2273 (2020).
13. B. Anasori, M. R. Lukatskaya, and Y. Gogotsi, "2D metal carbides and nitrides (MXenes) for energy storage," *Nat. Rev. Mater.* **2**, 16098 (2017).
14. Y. Dong, S. Chertopalov, K. Maleski, B. Anasori, L. Hu, S. Bhattacharya, A. M. Rao, Y. Gogotsi, V. N. Mochalin, and R. Podila, "Saturable absorption

- in 2D Ti_3C_2 MXene thin films for passive photonic diodes,” *Adv. Mater.* **30**, 1705714 (2018).
15. X. Jiang, S. Liu, W. Liang, S. Luo, Z. He, Y. Ge, H. Wang, R. Cao, F. Zhang, Q. Wen, J. Li, Q. Bao, D. Fan, and H. Zhang, “Broadband nonlinear photonics in few-layer MXene $\text{Ti}_3\text{C}_2\text{T}_x$ ($T = \text{F}, \text{O}, \text{or OH}$),” *Laser Photonics Rev.* **12**, 1700229 (2018).
 16. K. Hantanasirisakul and Y. Gogotsi, “Electronic and optical properties of 2D transition metal carbides and nitrides (MXenes),” *Adv. Mater.* **30**, 1804779 (2018).
 17. M. Naguib, M. Kurtoglu, V. Presser, J. Lu, J. J. Niu, M. Heon, L. Hultman, Y. Gogotsi, and M. W. Barsoum, “Two-dimensional nanocrystals produced by exfoliation of Ti_3AlC_2 ,” *Adv. Mater.* **23**, 4248 (2011).
 18. Z. Niu, T. Feng, K. Yang, T. Li, J. Zhao, G. Li, D. Li, S. Zhao, X. Jiang, H. Zhang, W. Qiao, H. Chu, and J. Lian, “MXene $\text{Ti}_3\text{C}_2\text{T}_x$ ($T = \text{F}, \text{O}, \text{or OH}$) saturable absorber for a 2 μm doubly Q-switched laser with AOM,” *Opt. Laser Technol.* **134**, 106642 (2021).
 19. Y. Zu, C. Zhang, X. Guo, W. Liang, J. Liu, L. Su, and H. Zhang, “A solid-state passively Q-switched Tm,Gd:CaF₂ laser with a $\text{Ti}_3\text{C}_2\text{T}_x$ MXene absorber near 2 μm ,” *Laser Phys. Lett.* **16**, 015803 (2019).
 20. H. Huang, J. Wang, N. Xu, S. Liu, G. Liang, and Q. Wen, “ Ti_2CT_x MXene as a saturable absorber for passively Q-switched solid-state lasers,” *Polymers* **13**, 247 (2021).
 21. G. Li, T. Li, W. Qiao, T. Feng, C. Feng, J. Zhao, G. Li, and S. Zhao, “Passively Q-switched Er:Lu₂O₃ laser with MXene material $\text{Ti}_4\text{N}_3\text{T}_x$ ($T = \text{F}, \text{O}, \text{or OH}$) as a saturable absorber,” *Opt. Lett.* **45**, 4256 (2020).
 22. C. Feng, W. Qiao, Y. Liu, J. Huang, Y. Liang, Y. Zhao, Y. Song, and T. Li, “Modulation of MXene Nb_2CT_x saturable absorber for passively Q-switched 2.85 microm Er:Lu₂O₃ laser,” *Opt. Lett.* **46**, 1385 (2021).
 23. W. Huang, C. Ma, C. Li, Y. Zhang, L. Hu, T. Chen, Y. Tang, J. Ju, and H. Zhang, “Highly stable MXene (V_2CT_x)-based harmonic pulse generation,” *Nanophotonics* **9**, 2577 (2020).
 24. Y. J. Sun, C. K. Lee, J. L. Xu, Z. J. Zhu, Y. Q. Wang, S. F. Gao, H. P. Xia, Z. Y. You, and C. Y. Tu, “Passively Q-switched tri-wavelength Yb³⁺:GdAl₃(BO₃)₄ solid-state laser with topological insulator Bi₂Te₃ as saturable absorber,” *Photonics Res.* **3**, A97 (2015).
 25. H. Kim, Z. Wang, and H. N. Alshareef, “MXetronics: electronic and photonic applications of MXenes,” *Nano Energy* **60**, 179 (2019).